

Reevaluation of Late Pleistocene loess profiles at Remizovka (Kazakhstan) indicates the significance of topography in evaluating terrestrial paleoclimate records

Tobias Sprafke^{a*}, Kathryn E. Fitzsimmons^b, Christoph Grützner^{c,d}, Austin Elliot^e, Laurent Marquer^{b,f}, Saida Nigmatova^g

^aInstitute of Geography, University of Bern, Hallerstrasse 12, 3012 Bern, Switzerland

^bResearch Group for Terrestrial Palaeoclimates, Max Planck Institute for Chemistry, Hahn-Meitner-Weg 1, 55128 Mainz, Germany

^cCOMET, Bullard Laboratories, Cambridge University, Madingley Road, Cambridge, CB3 0EZ, United Kingdom

^dFriedrich Schiller University Jena, Institute of Geological Sciences, Burgweg 11, Jena, Germany

^eCOMET, Dept. of Earth Sciences, Oxford University, South Parks Road, Oxford, OX1 3AN, United Kingdom

^fLaboratoire Géographie de l'environnement, Université de Toulouse Jean Jaurès, GEODE UMR 5602, Toulouse, France

^gInstitute of Geological Sciences K. Satpaeva, Ministry of Education and Science of Kazakhstan, 69A Kabanbay Batyra St. #279, 050010 Almaty, Kazakhstan

(RECEIVED April 30, 2017; ACCEPTED November 1, 2017)

Abstract

We report on a loess-paleosol sequence (LPS) near Remizovka, located in the northern Tian Shan piedmont of southeastern Kazakhstan. This site represents a key record for Late Pleistocene climatic fluctuations at the intersection of major northern hemisphere climate subsystems. This paper develops a synthesized dataset of previous conflicting studies at Remizovka by characterizing their (paleo)topographic context, which had remained previously overlooked. Digital elevation models, satellite images, and archival photography characterize recent topographic developments. Two well-developed pedocomplexes, which we investigate in detail and date by luminescence mark the paleotopography during Marine Oxygen Isotope Stage (MIS) 5. Peak dust accumulation rates here occurred during the middle MIS 5 and MIS 4/early MIS 3. These are partially comparable with records from neighboring regions, but not in phase with global ice volume records. This discrepancy may be related to a distinct regional environmental response to larger-scale climatic drivers and local topographic influences on dust deposition patterns. Our findings confirm the potential of the LPS Remizovka to provide high-resolution paleoclimate data for the Late Pleistocene. The three-dimensional stratigraphic reconstruction reinforces the caution required to correctly interpret loess formation processes prior to their interpretation as paleoclimate archives, and provides guidelines for a more suitable approach.

Keywords: Loess; Paleosol; Paleotopography; Paleoenvironment; Tian Shan piedmont; Central Asia

INTRODUCTION

Loess-paleosol sequences (LPS) reflect complex geoecological responses to climatic shifts across millennial and longer timescales, and provide quasi-continuous information relating to paleoenvironmental conditions during the Quaternary (e.g., Bronger, 1976; Dodonov and Baiguzina, 1995; Antoine et al., 2009; Sun et al., 2010; Fitzsimmons et al., 2012; Buggle et al., 2013; Zech et al., 2013; Marković et al., 2015; Sprafke, 2016). LPS are widespread across the mid-latitudes

and usually involve investigation of vertical exposures, which are assumed to be representative of the wider region.

Regional climate and geomorphic factors, as well as local topography, influence the development of LPS (Ruhe et al., 1967; Lehmkuhl et al., 2016). The presence of discontinuities and polygenetic units within LPS requires a reliable chronological framework combined with thorough genetic reconstructions of the interplay between aeolian deposition, pedogenesis, erosion, and colluviation (Sprafke et al., 2014; Sprafke, 2016). Recent advances in luminescence dating have improved our ability to unravel complex terrestrial paleoclimatic archives such as LPS (Stevens et al., 2007; Roberts, 2008; Thiel et al., 2011; Buylaert et al., 2012b; Jain et al., 2015; Ankjærgaard et al., 2016) by facilitating reliable correlations among units. The increasing application

*Corresponding author at: Institute of Geography, University of Bern, Hallerstrasse 12, 3012 Bern, Switzerland. E-mail address: tobias.sprafke@giub.unibe.ch (T. Sprafke).

of luminescence-based chronostratigraphies highlights the pitfalls of the simplistic correlation of paleosols or parameter variations in LPS and their correlation with global to hemispheric paleoclimate records (Vandenberghe et al., 2006; Rousseau et al., 2007; Schirmer, 2012; Li et al., 2016b). Most reliable correlations appear possible at loess plateaus with largely horizontal units (Kukla et al., 1990; Ding et al., 2002a; Marković et al., 2015), or at records created by large amounts of windblown dust (Antoine et al., 2009). However, even in these exceptional settings this approach needs to be applied with caution (Stevens et al., 2007). The rule to these exceptional settings are complex LPS, with their distribution and completeness largely depending on the topographical position.

To date, continental scale correlations of LPS across Eurasia that involve Central Asian records have mainly relied on pedostratigraphy (Bronger, 2003). Further large-scale approaches have been limited to regions with an established array of published records, such as in the Chinese Loess Plateau (CLP) or southeast Europe (Marković et al., 2015, 2016). The lack of long, investigated records from the intervening locations in Central Asia (Fig. 1A) is noteworthy. This lack of correlative data exists despite the widespread presence of loess deposits along the margins of the high mountain systems extending from Iran to Mongolia, with some deposits exceeding 100 m in thickness (Dodonov, 1991; Dodonov and Baiguzina, 1995; Bronger et al., 1998b; Ding et al., 2002b; Dodonov et al., 2006; Li et al., 2015). The limited amount of scientific studies in the region, and a distinct spatiotemporal pattern of aeolian dynamics (Smalley et al., 2006), has resulted in a lack of consensus about the

spatial pattern of climatic and geomorphic changes across the region (Machalett et al., 2008; Song et al., 2014; Kang et al., 2015; Li et al., 2015, 2016a; Vlamincx et al., 2016; Lauer et al., 2017; Fitzsimmons et al., in press). The growing number of publications related to the terrestrial paleoclimatic records of the Tian Shan piedmont (Fig. 1B) indicates an increasing scientific attention to this region located at the intersection of major climate drivers (i.e., westerlies, Asian monsoon systems, polar northerlies; Fig. 1A).

The classic model of loess formation for the region involves glaciofluvial transport of mountain sediments into the desert basins to the north, and the aeolian entrainment and transport of silt particles back to the foothills (Smalley and Krinsley, 1978; Dodonov, 1991). Comparisons with other regional paleoclimatic records suggest that the landscape change in the region is strongly driven by moisture availability. This includes glacial advance during wetter conditions, which facilitated loess generation (Koppes et al., 2008; Owen and Dortch, 2014). This response diverges from the mid-latitude model of loess deposition being mainly related to cold temperatures. Consequently, the utility of loess deposits as unambiguous responses to global paleoclimate shifts, and the scarcity of other, unambiguous paleoclimatic records in the region, highlights the need for detailed studies on local LPS.

Large-scale loess maps in the literature that cover Central Asia (Machalett et al., 2006; Song et al., 2012) indicate the approximate regional extent of these deposits. The variability in distribution and thickness of loess deposits along the piedmont, and the influence of pre-existing topography on loess accumulation, is unclear. Piedmont loess deposits may

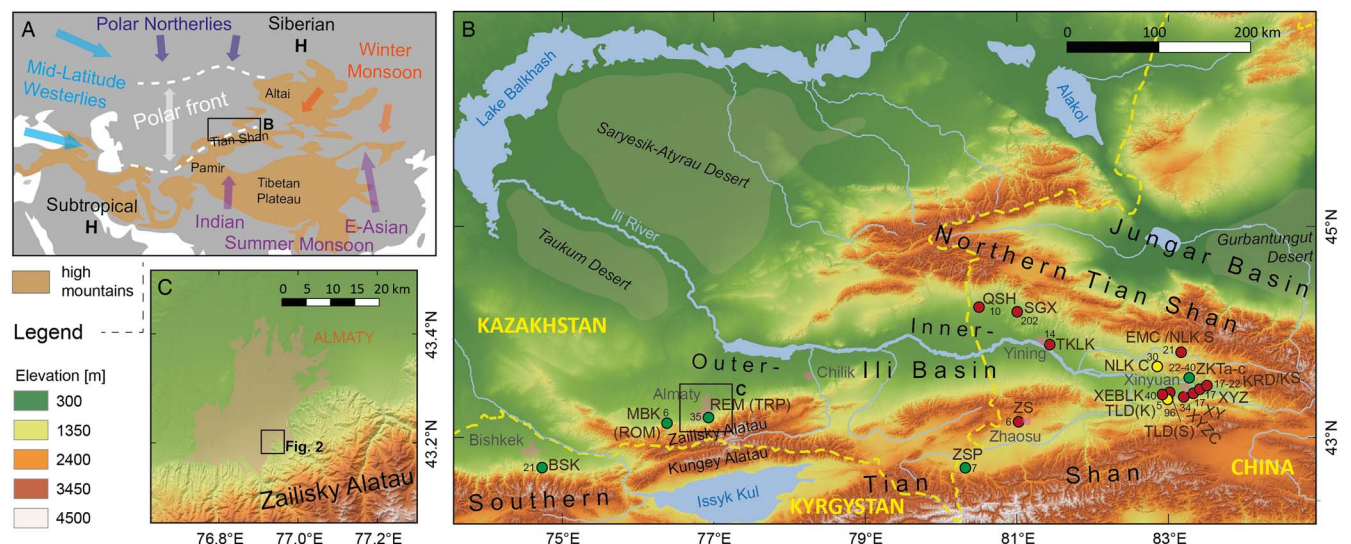


Figure 1. Geographic context of the LPS Remizovka. (A) Simplified map of Central Asia and surrounding regions illustrating the location of the Tian Shan piedmont LPS, at the intersection of important climate subsystems (cf. Machalett et al., 2008; Kang et al., 2015). (B) Locations and depths of LPS within the Ili-Balkhash catchment. Compiled from our own data and various references (Chen et al., 2012; E et al., 2012; Song et al., 2012, 2014; Youn et al., 2014; Kang et al., 2015; Song et al., 2015; Li et al., 2016a, 2016b). Due to missing or imprecise coordinates for several sites, three precision confidence classes are shown (red, = low; yellow = intermediate; green = high). Red signatures indicate information from sketch maps. For more information, refer to the .kmz-file provided in the supplementary information. (C) Topographic context of the Remizovka loess hill within the city of Almaty in the Zailisky Alatau (Southern Tian Shan) piedmont hills. (For interpretation of the references to color in this figure legend, the reader is referred to the web version of this article.)

be (1) blankets covering the preexisting topography, i.e., fluvial dissected foothills; (2) small loess plateaus dissected by high gradient streams and alluvial fans; and/or (3) in very rare cases positive landforms created by preferential dust deposition or erosion. Studies of vertical profiles must verify firsthand the internal structure of the deposits. Only then can paleoclimatic conditions and regional aeolian dust mass accumulation rates reliably be calculated.

In this paper, we present data from a loess section at Remizovka in southeastern Kazakhstan. This site is a >100 m wide section cut through a piedmont loess hill in the southern suburbs of Almaty (Fig. 1C) and our work represents a case study for the importance of understanding the landscape context of terrestrial paleoclimatic archives. Published studies of the site (Machalett et al., 2006, 2008; Fitzsimmons et al., in press), also known as Trampolin (Feng et al., 2011; Ran and Feng, 2014), have yielded contradictory results relating to its chronology, stratigraphy, and paleoenvironmental implications (see section The LPS Remizovka). In order to reconcile these disparate datasets, we undertook a detailed study of two prominent paleosols at the site. Their distinct paleotopography and a detailed investigation of the present site topography provides the missing link to integrate previous results. Our interpretations provide further paleoenvironmental conclusions and form the basis for future investigations on this potential key paleoclimatic archive for the wider region. Finally, we discuss the implications of our study with respect to the influence of local topography on the formation of LPS.

REGIONAL SETTING

Loess records along the Tian Shan range front

Relatively few terrestrial paleoclimatic records have been studied in Central Asia, as compared to Europe or China. Substantial areas of this region are marked by large temperate (semi-) deserts that are still not easy accessible, for both geographical and political reasons. In their study of the LPS Remizovka, Machalett et al. (2008) highlighted the importance of paleoclimatic studies within this region, because it lies at the intersection of major climatic subsystems (Fig. 1A).

Grain size variations from continuously sampled LPS in the wider region have been interpreted to reflect the dominant influence of the Westerlies in the Pamir (Vandenbergh et al., 2006) and Tian Shan loess deposits (Li et al., 2016b). Furthermore, the extreme continental climate with hot summers and cold winters results in large annual north-south shifts of the polar front (Fig. 1A). Machalett et al. (2008) reconstructed variations in the extent of polar front oscillations during the Late Pleistocene from the LPS Remizovka in the Zailisky Alatau foothills of the northern Tian Shan. To date, studies on Central Asian LPS exist largely independent of each other and only recently have attempts been made to investigate the timing and mechanisms responsible for silt production and deposition along the Tian Shan range front as a whole (Li et al., 2015, 2016a; Fitzsimmons et al., in press).

Several recent studies published from LPS in the eastern (Chinese) part of the Ili Basin (Fig. 1B) provide evidence for variable peak dust accumulation rates during marine isotope stage (MIS) 4 to early MIS 3 (Li et al., 2016a), middle MIS 3 (Song et al., 2015), and especially during MIS 2 (Li et al., 2016b). This variability strongly suggests a need to reconsider the spatiotemporal variations of dust deposition in higher detail before general paleoclimatic conclusions can be drawn. Crossing the border westwards into Kazakhstan, there is only a handful of international publications available from the Tian Shan piedmont loess (Machalett et al., 2006; Machalett et al., 2008; Feng et al., 2011; Ran and Feng, 2014; Fitzsimmons et al., in press). These studies likewise contain contradictory information. In most of these publications, not only the regional geomorphic context (Fig. 1B), but also the local scale (paleo)topography remained overlooked in the interpretation of continental scale paleoclimatic records present in the LPS.

Although no detailed maps of loess distribution and thickness exist for the Zailisky Alatau range front, our own field observations indicate that loess is not distributed continually along its length. Instead, loess deposits are partly interlayered by mountain debris. Only rarely do pure aeolian silt deposits in this area reach sufficient thickness for meaningful paleoclimatic studies (Sprafke and Obrecht, 2016). As reported for the Ili basin (Song et al., 2014), thick loess deposits along the Zailisky Alatau are located in various morphological positions, including sediment drapes on the foothills (e.g., Remizovka), in areas infilling mountain valleys (e.g., Maibulak), and as blankets of variable thickness on the plains in front of the range (e.g., along the highway westward from Almaty).

The active seismic setting of the Zailisky Alatau further complicates the pattern of loess distribution. The Zailisky Alatau is bound by a range front fault to the north, along which the mountains have overridden the foreland sediments. The fault's slip rate is not well established. In the easternmost part of the range front near Chilik, Selander et al. (2012) estimated a slip rate of 0.8 ± 0.5 mm/yr and 0.43 ± 0.3 mm/yr for two parallel faults, respectively. Apart from this main fault, several smaller faults of unknown activity are reported from Almaty and adjacent areas (e.g., Atrushkevitch et al., 1988; Delvaux et al., 2001), but no surface rupturing earthquakes are known for areas close to the study area. Severe earthquakes affecting the city of Almaty in the 19th and 20th century resulted from more distant epicenters or did not leave surface ruptures (Tatevossian, 2007; Abdrakhmatov et al., 2016; Landgraf et al., 2016).

The LPS Remizovka

In this paper, we address problems relating to the study of complex terrestrial paleoclimatic archives preserved in the Tian Shan piedmont loess, using the case study of Remizovka, the thickest known LPS of the Kazakh Tian Shan piedmont. This site has already been studied in detail (Machalett et al., 2006; Machalett et al., 2008; Feng et al.,

2011; Fitzsimmons et al., in press). It is located at ca. 1040 m above sea level (asl) on a north-northwest striking spur within piedmont hills along the southern margins of Almaty (Fig. 1C and 2). The hill is widely known for the modern ski jump facilities (Russian: *trampolin*) at the northern slope.

The present climate of Almaty is strongly continental. Mean annual precipitation and temperature are 580–680 mm and 8.5–10.0°C, respectively, depending on data source (Machalett et al., 2006; Weather and Climate, 2017), observation period, and altitude. Very cold winters and hot summers, and a precipitation maximum in spring and a secondary peak in autumn are typical. There is an altitudinal

gradient from the semi-desert (< 600 m asl) to steppe and shrub-steppe within the piedmont hills to the forest zone above ca. 1200 m asl.

Urban development along the southern margins of the city over the last few decades has resulted in substantial anthropogenic transformations at the Remizovka site (Fig. 2 and 3). Quarrying and the construction of ski jump facilities led to an exposure of several outcrops on different levels (Fig. 3 and 4A), including a ca. 30 m high loess exposure at the hilltop (Fig. 4B) and several outcrops at a lower level (Fig. 4A and 4C). Since 2015, the additional construction of a racing track below the main cliff and around

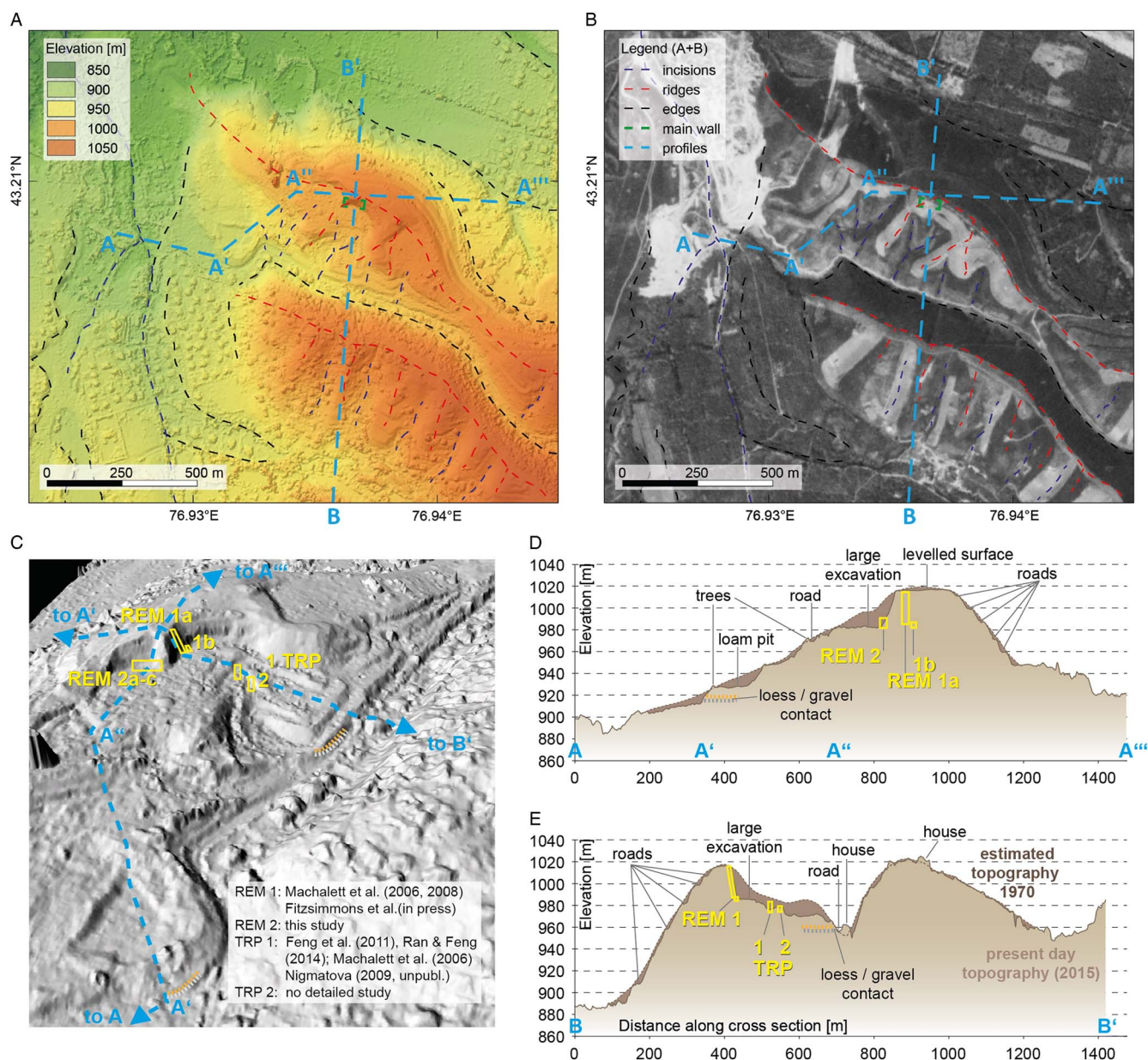


Figure 2. (color online) Topography of the Remizovka loess hill. (A) Digital elevation model (DEM) based on the Pléiades dataset, locations of cross sections (Fig. 2D and E), and characteristic features visible in Fig. 2B. (B) Corona declassified satellite image from 1969. (C) Three-dimensional visualization of the loess hill based on the DEM and location of the profiles from previous works and this study. (D and E) Cross sections along the transects marked in Fig. 2A and B, including specific features and reconstruction of the topography before quarrying.

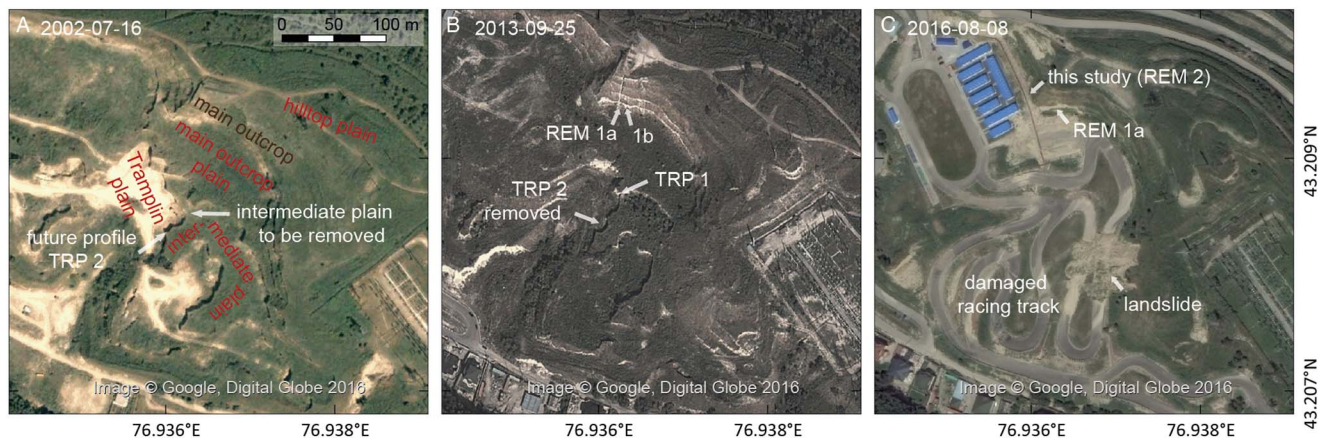


Figure 3. (color online) Human-induced changes to the Remizovka loess hill, as documented by pictures available on Google Earth. (A) Situation of the loam quarry in 2002, before the start of investigations. (B) Situation in 2013, with the profiles in the main section (REM 1a and b) and TRP 1. TRP 2 has already been removed by loam quarrying between 2010–2012. (C) Situation in 2016, with the location of the profile studied herein (REM 2). Note the loss of most sections below the main outcrop wall due to the construction of a racetrack and destruction caused by the collapse of disturbed loess material during heavy rains in spring 2016. For the full documentation refer to the complete set of images available on Google Earth.

the hill has removed the outcrops at the lower levels (Fig. 4D) and left only the main outcrop accessible for study (Fig. 4E and F, Fig. 5).

Machalett et al. (2006) estimated the thickness of the Remizovka section at 70–80 m, based on the composite stratigraphy (cf. Fig. 6A and 7) of three outcrops exposed at different altitudes down the loess hill, which overlies gravels. A photograph by Machalett et al. (2008) documents the upper part of this composite LPS, a 28.5 m thick profile dug into the main outcrop (Fig. 4B), and analyzed in 10 cm resolution for granulometric variations and ratios; these data were then interpreted as paleoclimatic proxies (Fig. 6A). According to Machalett et al. (2006), the entire LPS Remizovka covers more than seven glacial-interglacial cycles, correlating with long records in western Central Asia and China. However, non-fading-corrected feldspar infrared stimulated luminescence (IRSL) ages from the composite section never exceeded 100 ka.

Feng et al. (2011) worked on the 10.5 m thick Tramplin subsection on the mid-slope of the hill (Fig. 4A and C). Together with the study by Ran and Feng (2014), a multi-proxy dataset (Fig. 6B) and radiocarbon dates on snails and organic matter, ranging between ~32–46 cal ka BP, were published. In a palynological study of the same profile, Nigmatova (2009) detected numerous steppe species related to well-developed buried soils.

Fitzsimmons et al. (in press) worked on the upper 8 m of the trench dug into the main outcrop (Machalett et al., 2008; Fig. 4B). Their stratigraphic data, based on color variations, correlates well to the features described previously, and their luminescence ages indicate an age of < 35 ka for the upper 8 m of the profile (Fig. 6C). The new dataset supersedes the older, non-fading-corrected IRSL chronology of Machalett et al. (2006) but lies well within error of two radiocarbon dates from this section (Machalett et al., 2008).

After 10 years of research on the Remizovka loess hill, human activities seriously threaten the unique outcrop (Fig. 3C and 4D), demanding detailed studies and, in the best case, preservation as a geologic heritage (Vasiljević et al., 2014). Our field evidence indicates that two well-developed paleosols in the lower part of the main wall studied by us are not horizontal, but rather follow a distinct paleotopography (Fig. 4). In this paper, we aim to reconcile the previous works at this site by examining it in three-dimensional space, so as to better understand the role of local topography in the formation of this LPS.

METHODS

Field investigation and sampling

Access to the Remizovka loess hill in June 2016 enabled field observations and initial sampling. We traced two prominent pedocomplexes along the main outcrop (Fig. 4E and F). These are located between 22–24 m depth below the hilltop according to the profile of Machalett et al. (2008). Due to the short time of access allowed by the authorities, we could only dig three shallow profiles to expose the two paleosols and parts of the overlying and underlying sediments (Fig. 4F and 5).

Soil descriptions followed pedological designations (FAO, 2006) after Sprafke (2016), and previously applied to the upper 8 m of the LPS Remizovka (Fitzsimmons et al., in press). All sampling locations are shown in Figure 5. Two luminescence samples, taken to bracket the two paleosols, were collected in duplicate within lightproof tubes driven horizontally into the loess section. Additional material from the in situ sediment surrounding the tube samples was collected in sealed plastic bags for dose rate and moisture content determination and further analyses. In addition, three samples were taken from the most developed paleosol horizons.



Figure 4. (color online) Photos from the past (A–C) and present (D–F) outcrops at Remizovka. (A) Panorama photo from the Tramplin plain (ca. 2004) created from archival photography (S. Nigmatova). Note that the main outcrop plain and the majority of the main outcrop are not visible due to the perspective. The location of the two TRP profiles (1, 10.5 m thick; 2, 6.4 m thick) is marked. Note the dipping of a well-developed paleosol along the outcrop, most likely the MIS 5e paleosol. (B) Photo of the main outcrop in 2004 (S. Nigmatova) studied by Machalett et al. (2006). The long REM 1a profile is complemented by profile REM 1b a few meters to the right. (C) TRP 1 section (studied as Tramplin profile by Nigmatova, 2009; Feng et al., 2011; Ran and Feng, 2014; most likely the middle part of synthetic profile by Machalett et al., 2006). (D) Overview in June 2016 (cf. Fig. 3C). The studied sections are located behind the blue roof on the left hand side of the photo. (E) Detail of D, showing the dipping of the two well-developed paleosols to the west. (F) Studied section including the two well-developed paleosols and the complementary profiles REM 2a–c (Fig. 5).

Grain size and color analyses

Representative parts of the five disturbed samples were air-dried and sieved to fine earth (<2 mm). A ColorLite sph850 spectrophotometer (3.5 mm measuring field, D65 light source, 10° observation angle) determined the diffuse reflection spectrum (3.5 nm resolution, 400–700 nm), which is converted to variables of the CIELAB color space and visualized as RGB colors (Sprafke, 2016; Fitzsimmons et al., in press).

A Malvern Mastersizer 2000 Hydro S (refraction index 1.52, stirring speed of 2100 rpm, average of three 12 s measurements) was used to determine the grain size distribution

(104 classes, size range of 0.2–2000 μm). Before measuring, each sample (1.5 g) was mechanically split, using a rotary sample divider, until required obscuration was achieved.

Luminescence dating

Luminescence samples were processed at the Max Planck Institute for Evolutionary Anthropology, Leipzig (MPI-EVA), under filtered red light conditions and using the same approach as applied to samples from the upper parts of this section by Fitzsimmons et al. (in press). Published protocols were used to extract the fine-grained polymineral fraction of the samples for dating (Frechen et al., 1996). From each

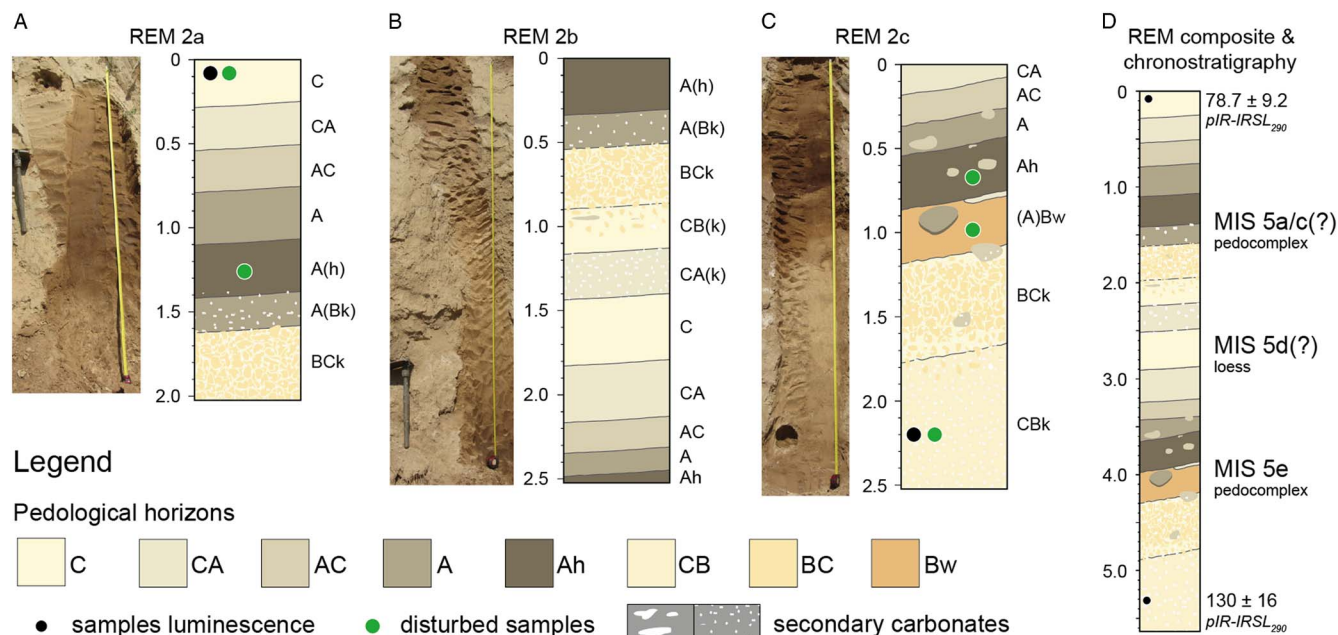


Figure 5. (color online) Field interpretations of the studied profiles and sampling positions: (A) REM2a, (B) REM2b, (C) REM 2c, and (D) composite sequence. Classification and legend based on FAO (2006) and Sprafke (2016).

sample, 18 aliquots were delivered by pipette onto stainless steel discs. Aliquots were measured for equivalent dose (D_e) on a Risø TL-DA-20 reader with D410 filters to detect the feldspar signal, using the post-infrared-infrared (pIR-IR₂₉₀) protocol (Buylaert et al., 2012a) to access the stable feldspar signal. Resulting D_e values were interpolated from exponential and linear fitting of the dose-response curves.

The luminescence samples appeared to respond well to the measurement protocols. No aliquots had reached saturation; for all aliquots, pIR₂₉₀ signals were bright; recycling ratios were within 5% of unity; sensitivity change lay within 30% of unity; residual dose was <1%. The Central Age Model (Galbraith et al., 1999) was used to calculate the D_e for each sample, since dose distributions were Gaussian in both cases (Supplementary Figure 1). Fading measurements following published guidelines (Auclair et al., 2003; Thiel et al., 2014) yielded fading rates (g_{2days}) below 1.5%/decade and comparable with published investigations into the pIR₂₉₀ signal (Buylaert et al., 2012a; Thiel et al., 2014), which indicate minimal fading. We did not correct the ages reported in Table 1.

Environmental radiation dose rates for beta and gamma components were derived from beta counting at the MPI-EVA, and high-resolution germanium gamma spectrometry undertaken at the Felsenkeller, VKTA Dresden, respectively. Published attenuation factors (Adamiec and Aitken, 1998), modelled moisture contents, and alpha-values of 0.12 ± 0.02 (Rees-Jones and Tite, 1997), were used to correct the beta and gamma components of the dose rate. Long-term moisture contents were modelled by taking into account in situ and saturation water content of those samples, as well as the in situ water content of the loess samples from the upper part of the profile (Fitzsimmons et al., in press), with respect to the likely periods of time over which different degrees of saturation were

likely to prevail. A large uncertainty was incorporated to account for variability in moisture content through time. Cosmic ray contributions to the total dose rate were calculated based on published formulae (Prescott and Hutton, 1994).

GIS analyses of DEMs

We used stereo Pléiades satellite imagery (November 2014) with a spatial resolution of 0.5 m to produce a high-resolution digital elevation model (DEM) of the study area. Stereo panchromatic photographs from the Pléiades platform capture the same area on the ground from two different angles which allows to reconstruct the three-dimensional geometry of the terrain (de Lussy et al., 2005). Data processing was undertaken with commercial software (ERDAS Imagine). The resulting DEM has a resolution of 1.5 m and was processed with standard GIS techniques to compute slope and hillshade. As reference for absolute altitudes and for the overview maps (Fig. 1B and C) we used NASA SRTM1 data (2000) with a horizontal ground resolution of 30×30 m.

Archival photos and historic satellite images of Google Earth® and Corona

To reconstruct the approximate positions of the previously studied profiles below the main outcrop, we referred to archival photos of co-author S. Nigmatova (summer 2004) and R. Iovita (summer 2013). In addition, using the Google Earth software, 33 satellite images from between 2002 and 2016 are available for comparison. Due to the steep slopes and different angles of observation, the georeferencing of Google Earth images is only approximate. Using ERDAS Imagine, we georeferenced several images in the best way

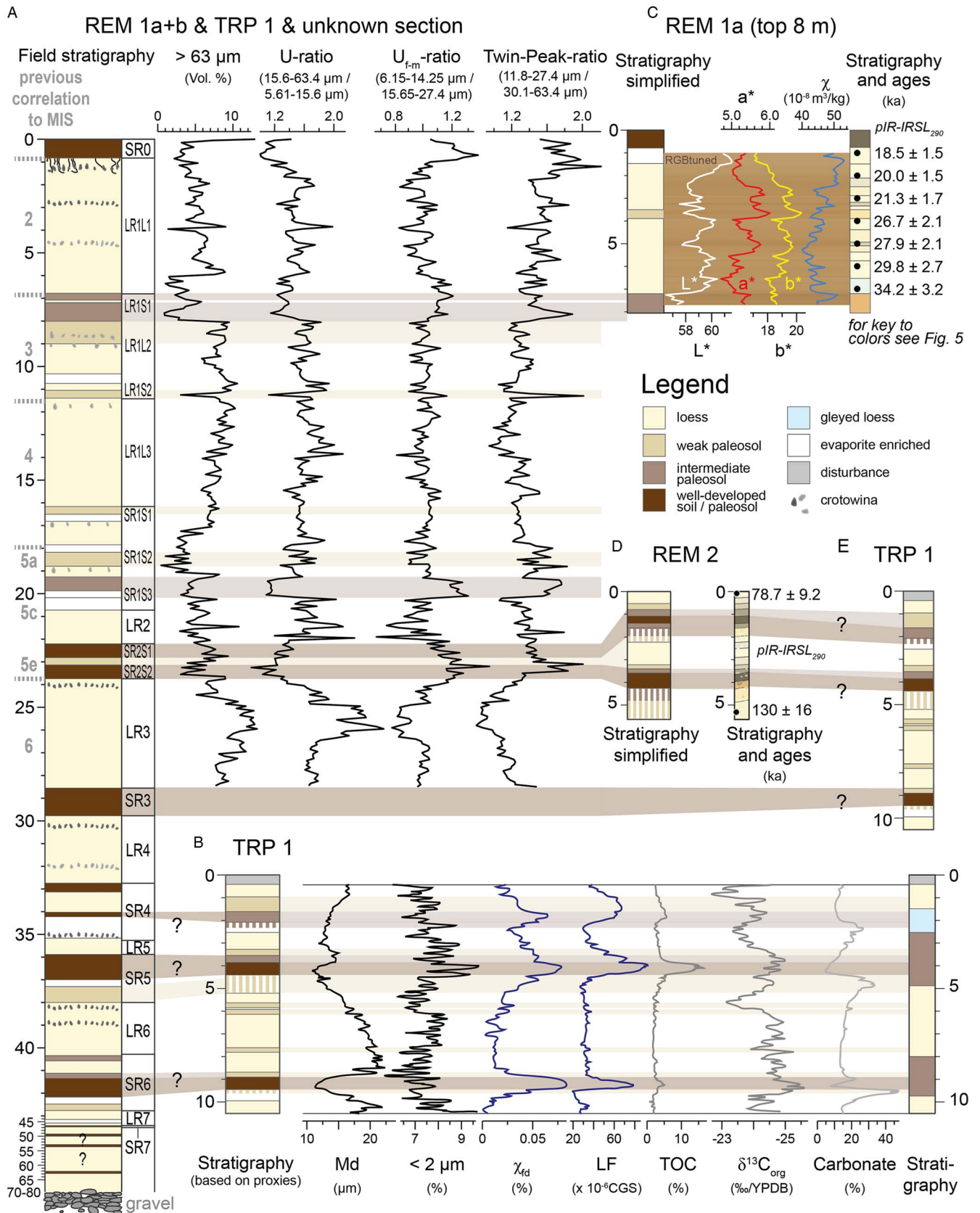




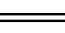


Figure 6. (color online) Compilation of profiles with simplified stratigraphies following a standardized legend, together with published and new data and their possible correlations. (A) Synthetic profile (redrawn from Machalett et al. 2006) with grain size data and correlation to marine isotope stages (redrawn from Machalett et al. 2008). (B) TRP 1 section with multiproxy dataset redrawn from Feng et al. (2011) and Ran and Feng (2014). Note the more detailed revised stratigraphy based on reinterpretation of the published data. (C) Upper part of REM 1a with color, magnetic susceptibility, and luminescence ages modified from Fitzsimmons et al. (in press). (D) New composite profile REM 2 (cf. Fig. 5) with luminescence ages. (E) Correlation of TRP 1 with composite profile REM 2.

Table 1. Color and granulometric data of selected horizons within the studied sequence. For the full data set, please refer to the supplementary information.

Pedological horizon	color				granulometry									
	L*	a*	b*	RGB	0-2 μm	2-4 μm	4-6.3 μm	6.3-20 μm	20-63 μm	63-125 μm	125-200 μm	9-28 $\mu\text{m}/$ 32-63 μm	Mean	Mode
CA	63.3	4.7	17.4		11.0	9.0	7.7	29.2	34.5	7.9	0.7	1.7	24.4	27.3
A(h)	51.9	6.5	16.4		13.2	11.2	9.7	34.0	27.6	4.2	0.2	2.6	18.2	18.0
Ah	43.0	7.0	14.9		14.6	11.9	9.8	32.5	26.3	4.7	0.1	2.5	18.1	17.3
Bw	48.5	8.5	19.1		14.0	11.1	9.4	32.2	28.2	5.1	0.0	2.3	18.9	18.6
CBk	66.2	5.1	16.5		15.2	9.8	7.9	30.0	30.2	6.4	0.4	2.1	21.1	21.8

available to document the history of loam quarrying, construction, and thus the conditions for previous scientific investigations. For comparison, a declassified monochromatic Corona KH-4B surveillance satellite photograph (ca. 1.8 m resolution) from 1969 is added to the time series (cf. Narama et al., 2010), to show the degree of least disturbance documented from the site.

RESULTS AND DISCUSSION

Investigations undertaken for this study address the contradictory results of previous studies. As our data link disparate chronostratigraphies, we discuss both our data and the reconstruction of past work together by (1) reconstructing the precise location of the previous studies, and how these specific sites may have been altered or removed from the exposure through construction activities; (2) investigating in detail the two pedocomplexes that serve as marker horizons along the main exposure face; (3) correlating the previously published stratigraphies to one another and to our data, so as to create a unified dataset; and (4) reconstructing the local topographic and environmental development of the Remizovka loess hill to understand how local paleotopographic conditions and processes may influence a loess paleoenvironmental archive. We will also reflect on the regional and methodological implications of this study.

Local topography and LPS exposure through time

Despite the relatively poor image quality, the Corona KH-4B image from 1969 (Fig. 2B) serves its purpose to evaluate the original topography before the period of significant quarrying activities (Fig. 2D and E). The Remizovka loess hill in 1969 had a topography comparable to the hill immediately to the south. Both formed spurs striking SE to NW, dissected by a valley. The slopes of the separated hills are asymmetric, with steeper north-facing slopes and gentler south-facing slopes dissected by small valleys (Fig. 2A and B).

Over 30 Google Earth images provide detailed information relating to human-induced changes on the Remizovka loess hill over the last 16 years (cf. Fig. 3). The satellite image from 2002 (Fig. 3A) shows the topography resulting from loess quarrying,

prior to any known scientific investigation (e.g., Machalet et al., 2006; Feng et al., 2011). One main outcrop wall and a few lower terraces are visible. In the following, we refer to these sites by the names given in Figure 3 (cf. Fig. 4). For all profiles, we use the names introduced in Figure 2 (cf. Fig. 4).

Archival photos by S. Nigmatova (Fig. 4A–C) document a field campaign during 2004, including the profiles dug into the Traplino outcrop (TRP 1 and 2) and the main outcrop (REM 1). Machalet et al. (2008) produced a photo of the main outcrop (their Fig. 4b, cf. Fig. 4B herein), with a 28.5 m thick profile (REM 1a) extending from the hilltop. An additional small profile (REM 1b) is exposed a few meters to the right.

Google Earth imagery shows that quarrying between 2010–2012 removed a >6 m thick loess profile. This profile was not studied in detail (TRP 2; cf. Supplementary Fig. S2). The >10 m high TRP 1 trench, ca. 35 m to the north and studied by Feng et al. (2011) together with S. Nigmatova, and most likely by Machalet et al. (2006), is still visible on the satellite image from 2013 (Fig. 3B) and an archival photo from the same year (Supplementary Figure 3). One year later, the construction of the racing track had removed most profiles below the main outcrop. Landslides during heavy rains in spring 2016 mainly removed loess sediments disturbed or relocated by human activities, causing severe damage to the racing track (Fig. 3C and 4D).

The Pléjades DEM (Fig. 2) provides unprecedented topographic detail and precision, albeit only for the date of measurement (November 2014). The DEM does not show the prominent terraces below the main wall, which were still visible on Google Earth imagery from early summer 2014, but absent by early summer 2015. This indicates that the substantial modification of the topography for the construction of the racing track had already started in summer/autumn 2014.

Figures 2 and 7 show topographic features and reconstructed topographies from 1969 and the mid-2000s, respectively, combining the data from the DEM derived cross sections and visual interpretation of aerial imagery. The hilltop plain is leveled, but the almost completely preserved steppe soil in the top of REM 1a (Machalet et al., 2006) indicates that minimal material was removed overall. The contact between loess and underlying gravels could be observed at different altitudes along the road in the valley

Table 2. Equivalent dose (D_e), dose rate data and luminescence age estimates for the Remizovka marker paleosol. D_e values, total dose rates (incorporating α -values of 0.12 ± 0.02 after (Rees-Jones and Tite, 1997)) and age estimates are based on polymineral pIR-IRSL₂₉₀. Dose rates are already attenuated for moisture content which for both samples was measured as $12 \pm 4\%$.

Sample code	Description	Depth (m)	De (Gy)	Overdispersion (%)	Dose rates (Gy/ka)					Age (ka)
					Gamma	Beta	Cosmic	Water content (%)	Total	
EVA1524	Above double paleosol	22.0 ± 0.5	423 ± 14	17	1.42 ± 0.16	3.16 ± 0.32	0.03 ± 0.00	12 ± 10	5.43 ± 0.42	78.7 ± 9.2
EVA1523	Below double paleosol	23.5 ± 0.5	571 ± 24	31	1.15 ± 0.13	2.46 ± 0.25	0.03 ± 0.00	13 ± 10	4.39 ± 0.35	130 ± 16

south of the Remizovka loess hill (Fig. 2C–E). The precise altitudes of the profiles below the main wall remain unclear and are approximated in the best way possible from the available images (Fig. 2–4, 7).

Properties and age of the two pedocomplexes in REM 2

Two highly visible paleosols from the lower part of the main outcrop (ca. 22–24 m below the hilltop in profile REM 1a) dip westwards. We investigated these at an outcrop (REM 2) where they are exposed at eye level from the main outcrop plain (Fig. 4E and F). Due to the steep dip angle, the outcrop was studied in three short subsections (REM 2a–c) that encompass the two paleosols.

Figure 5 shows profile photos, a pedological description, and a composite profile. The loess sediments below the lower pedocomplex are slightly darker and more structured (subpolyhedral) than typical primary loess and are visibly enriched in secondary carbonates (primarily pseudomycelia; BCK/CBK-horizons). The lower paleosol has a dark brown Ah-horizon and a brown Bw-horizon with a sharp lower boundary. The Ah-horizon grades into a 1 m thick package of partly humic loess with a gradual transition to well-structured (subpolyhedral) and more clayey loess, often with light-colored silty substrate between aggregates (CBK/BCK). This horizon is directly below the upper humic paleosol (A[h] horizon), which is lighter in color than the Ah-horizon of the lower pedocomplex. The transition to the overlying loess is gradual. As both of the well-structured BCK horizons are found below well-developed paleosols, we interpret both packages to be pedocomplexes.

Color data support the pedologic classifications made above (Table 1). Soil horizons yield low L^* (lightness) values, and the brown horizon the highest a^* (redness) and b^* (yellowness) values. The quantitative color data from the underlying and overlying loess horizons appear comparable to the primary loess sediments at the top of REM 1a (Fitzsimmons et al., in press). Although these were measured with a different spectrophotometer, it was from the same manufacturer; experience suggests that color values measured with different devices cannot necessarily be compared in absolute terms despite appropriate calibration.

Granulometric measurements indicate that clay content ($<2 \mu\text{m}$) is highest in the basal CBK-horizon (Table 1). This may be the result of post-depositional clay formation or fine carbonate impregnation. Taking into account that laser diffraction methods have difficulties in determining clay contents, some researchers suggest alternative upper boundaries for the clay fraction of $4.6 \mu\text{m}$ (Antoine et al., 2009) or even up to $8 \mu\text{m}$ (Konert and Vandenberghe, 1997). These would effectively reduce the relative dominance of clay in the lowermost horizon. Both the mean grain size and mode exceed $20 \mu\text{m}$ in the uppermost and lowermost horizons and are therefore clearly coarser than the paleosol horizons.

As our analyses do not reveal the twin peak in grain size distribution observed by Machalett et al. (2008), we use the ratio of $9\text{--}28 \mu\text{m}/32\text{--}63 \mu\text{m}$ as an approximation. The ratio of grains within these classes, rather than the gap in between, appears more likely to reflect paleoenvironmental changes recorded by granulometric variations. The general tendency of higher values within the pedocomplexes is similar. However, it is difficult to compare our results to the data of Machalett et al. (2008), which were obtained by a Beckmann Coulter LS 13320 PIDS laser instrument, due to the unclear precise stratigraphic relation and differences in specifications of the two laser diffraction devices used (Schulte et al., in press).

Age estimates for the two luminescence samples and relevant additional dating information are provided in Table 2. The ages are consistent with depth and stratigraphy, and constrain the timing of significant pedogenesis to between $78.7 \pm 9.2 \text{ ka}$ and $130 \pm 16 \text{ ka}$. This interval most likely corresponds to MIS 5.

Chronostratigraphy of the main outcrop (profiles REM 1 and 2)

Fitzsimmons et al. (in press) investigated the upper 8 m of the REM 1a profile (Machalett et al., 2008); it is clear that this section does not directly correlate their profile to REM 2. The two pedocomplexes studied here at REM 2 are visible along the lower third of the main outcrop, and can be followed with confidence along the outcrop. They correspond to the double paleosol (SR2) described by (Machalett et al., 2006). Their SR2 consists of two Bt horizons separated by a 35 cm thick

loess unit. The different topographic position provides a reason for the increased thickness of loess between the studied pedocomplexes in REM 2, but not for the difference in our pedological interpretations. Machalett et al. (2006) do not mention humic/cambic horizons. Their Bt horizons most likely correspond to the well-structured BCk horizons in REM 2. However, these horizons lack clay coatings and other characteristics of Bt horizons developed in loess, namely (dark) brown color, (sub)polyhedral structure or often an underlying Ck horizon (Bronger, 1976; Sedov et al., 2013). The paleosols of SR2 at REM 1 are unlikely to be Bt horizons, since fundamental changes in soil forming factors could not have occurred across such short distances.

The ages we report for the two pedocomplexes at REM 2 (constrained to between 78.7 ± 8.2 ka and 130 ± 16 ka) agree with the general stratigraphic assumptions of Machalett et al. (2008), who assumed formation of their SR2 during MIS 5 based on amino acid racemization (AAR) dates. However, this leaves insufficient time for the formation of the SR1 complex during MIS 5, and requires parts of it to have formed during MIS 4. It would be an over-interpretation to correlate the two studied pedocomplexes (SR2) to the three “warm” marine isotope stages during MIS 5. It is unclear if the LPS Remizovka records a distinct paleoenvironmental response to global climatic changes, which differs from LPS at the Chinese loess plateau (Kukla, 1987; Ding et al., 2002a; Porter, 2013) and Europe (Marković et al., 2011).

It remains to be established if the primary loess deposition phase between the two pedocomplexes occurred during MIS 5d or 5b, or if it corresponds to any relative peaks in the global ice volume. A detailed geochronological study is as yet only available for the upper 7 m of REM 1a. Taking the revised numerical ages by Fitzsimmons et al. (in press) into account, a substantial part of this 28.5 m thick profile (ca. 6–20 m depth) corresponds to MIS 4 and MIS 3. The D/L ratio of glutamic acid determined through AAR by Machalett et al. (2008) shows a distinct plateau from 10–20 m depth. The peak of dust accumulation at Remizovka would therefore most likely correspond to MIS 4–early MIS 3, which differs from most records in Europe and the Chinese Loess Plateau.

The Tramplin profiles (TRP 1 and 2) and their relation of the main outcrop (REM 1 and 2)

According to archival photography from the Tramplin outcrop, Machalett et al. (2006) did fieldwork on the TRP 1 section (Fig. 4C), which was studied in detail by Feng et al. (2011) and Nigmatova (2009). The relationship of this profile to their synthesized standard stratigraphy is not clarified in their publication.

The high-resolution multiproxy study by Feng et al. (2011) focused on chronostratigraphy, and therefore lacks discussion of their detailed dataset on magnetic susceptibility, granulometry, carbonate content, and organic carbon. We interpret these parameter variations (also Ran and Feng, 2014) as valuable indicators of changes in the balance

between aeolian sedimentation and pedogenesis. High magnetic susceptibilities, high clay contents, high organic matter contents, together with low amounts of carbonate, all indicate intensive pedogenesis (oxidation, humification, hydrolysis, and carbonate leaching, respectively). Horizons below the paleosols are commonly enriched in leached carbonates, which is also consistent with well-developed soil profiles. Our reinterpretation of the data suggests a subdivision of the profile studied by Feng et al. (2011) into three moderately to well-developed paleosols (Fig. 6B). Based on this reinterpretation, the stratigraphic succession at the TRP 1 profile closely matches the succession occurring between 33–42 m in the synthesized stratigraphy of Machalett et al. (2006). We therefore assume that Machalett used the same profile for his publication as Feng (TRP 1, Fig. 6A and B).

The archival photos in Figures 4A and C show a well-developed paleosol in the upper part of the TRP 1 profile, which probably represents the paleosol identified at 4 m depth from the data of Feng et al. (2011). Surprisingly, the stratigraphy of the TRP 1 profile *also* matches the succession exposed at REM 2, with only slight deviations in the thickness of the loess packages (Fig. 6D and E). On this basis we can conclude that the TRP 1 profile correlates either to the succession in REM 2 (MIS 5) or to an even older part of the LPS Remizovka, but not to the last full glacial cycle. The chronological framework for the TRP 1 section (Feng et al., 2011) was based on radiocarbon dating of snails and organic matter and suggests an age range of ca. 32–46 ka. Given the two possibilities for correlation with the REM 1 and REM 2 sections, this chronology is likely to be unreliable, for two reasons. Firstly, the degree of pedogenesis of the three paleosols is significant and unlikely to have occurred during such a short period during MIS 3. Secondly, apparent plateauing of radiocarbon dates based on bulk organics, yielding apparently younger chronologies than should be the case compared with independent methods, is known to occur. In particular, Song et al. (2015) observed a plateau in radiocarbon dates beyond a certain depth within Ili basin loess profiles, compared with an independent chronology using luminescence ages that continued to increase with depth. The authors explain this phenomenon by modern carbon contamination. The controversy related to the dating of the Paudorf soil (Lower Austria) is one example outside the study region, where radiocarbon dating produced numerical values from charcoal far beyond the dating range of this method (Vogel and Zagwijn, 1967; Fink, 1976; Sprafke, 2016).

Nigmatova (2009) analyzed the pollen assemblage of 67 samples covering the whole TRP 1 profile. Peaks in pollen abundance at 1.0–2.0 and 3.5–5.0 m depth correspond well to the two paleosols in the upper part of TRP 1. The primary loess sediments do not contain significant amounts of pollen. The pollen spectra indicate the dominance of steppe species during MIS 5. Organic material is well preserved within the rather old humic paleosols in this otherwise semi-arid, strongly continental environment, and bodes well for future work based on organic proxies.

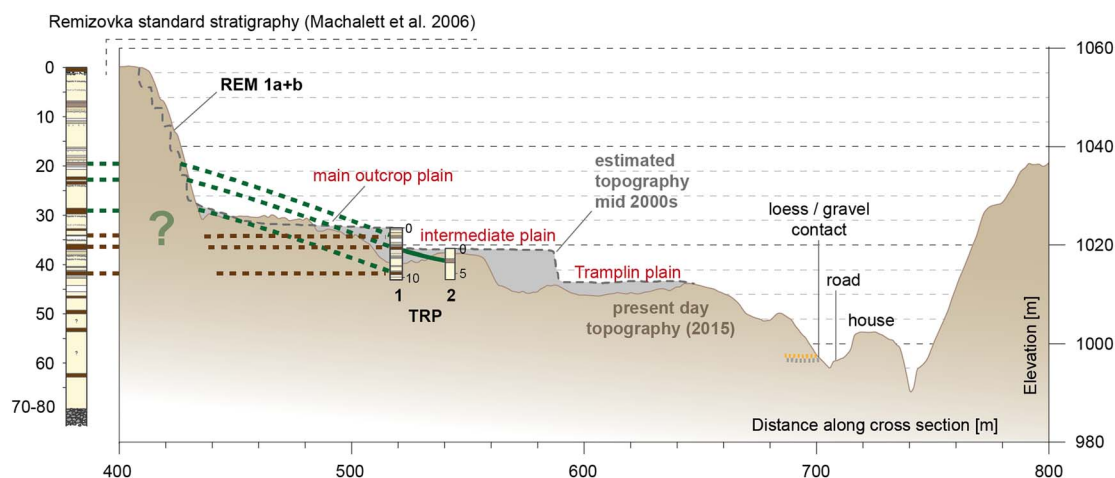


Figure 7. (color online) Detail of transect B-B' (cf. Fig. 2) and relation between previously studied profiles. The conceptual model of plateau-like dust deposition at Remizovka (with later fluvial incision) leads to the assumption that TRP 1 represents the second part of the composite profile Remizovka (Machalett et al. 2006; red dashed lines). Our scenario (green dashed lines) involves a hilly paleotopography, with TRP 1 correlating to the lower part of REM 1 (and with its upper half to REM 2, studied by us). (For interpretation of the references to color in this figure legend, the reader is referred to the web version of this article.)

Fieldwork at the adjacent TRP 2 section did not lead to a further publication, but the photographic documentation is useful to resolve uncertainties related to the paleotopography recorded at Tramplin. The paleosol at 4 m depth in TRP 1 is clearly visible along the uncleaned outcrop in the photograph provided (Fig. 4A and C) and leads into profile TRP 2 (with the top ca. 4 m lower than TRP 1) at a depth of 2 m. This indicates an overall inclination of ca. 6 m over a lateral distance of ca. 35 m.

Based on published data, including archival photography, and our own work, we infer that all studied sections—REM 1 and 2 and TRP 1 and 2—encompass the same SR2 pedocomplex corresponding to MIS 5. REM 1a covers a well-resolved LPS from MIS 1 through to the primary loess of MIS 6. The TRP 1 profile (Feng et al., 2011) most likely exposes most of the MIS 5 record in the upper half of the profile (SR2), and includes an older paleosol at the base, which was probably exposed at REM 1b and likely corresponds to the SR3 of Machalett et al. (2006). The sequence investigated by Machalett et al. (2006) therefore comprises a synthesized composite of three sections, each successively lower in the landscape (Fig. 7). The assumption made during their study, not substantiated by more extensive field survey or drilling, was that the stratigraphy recorded in each section naturally overlies, and does not overlap with, the underlying exposure (dark red dashed lines in Fig. 7). The authors appear to have assumed a plateau-like context for loess accumulation at Remizovka, with the profile at the lower outcrop (TRP 1) complementing the upper profiles (REM 1a and b). Based on the close correlation of physical characteristics and the likely location of the second stage of the synthesized profile (Machalett et al., 2006), we suggest that the second, middle profile (TRP 1) replicates the lower part of the main REM 1 profile. In addition to the lack of fading correction, this may explain

why the numerical ages reported by Machalett et al. (2006) never exceed 100 ka.

Local paleotopography and –environmental development at Remizovka

According to our reinterpretation of the stratigraphy, the SR2 paleosol of Machalett et al. (2006) marks the surface of a paleo-hill present during MIS 5. The dip in stratigraphy from REM 1a westwards to REM 2 is clearly visible in the exposed outcrop (Fig. 4E). Consequently, we may also assume a southward dip in paleotopography from REM 1 towards the TRP profiles (green dashed line on Fig. 7), consistent with the dipping visible in the Tramplin outcrop on the photo from 2004 (Fig. 4A). Despite recent alteration and removal of the Tramplin outcrop at Remizovka, and the distinct paleotopographic development, it is nevertheless possible to reconstruct the general stratigraphy of the locality and reconstruct local paleoenvironments and topographies in three dimensions, back through time.

The paleotopography preceding and during the very first phases of loess accumulation at Remizovka is not clear. Due to the as yet undefined paleotopography below the sections investigated here, we cannot estimate the total thickness of the loess deposit at Remizovka simply based on the elevation of the contact of loess and the underlying gravels (Fig. 2). Estimates exceeding 70–80 m (Machalett et al., 2006) are likely exaggerated. Given the uncertainties in correlating paleosols at Remizovka with marine isotope stages, it is unclear if the well-developed paleosol in the lower part of the TRP 1 profile (Feng et al., 2011), the SR3 of Machalett et al. (2006), corresponds to MIS 7. The comparable thickness of loess between SR3 and SR2 both at REM 1 and TRP 1 indicates that loess accumulation during MIS 6 appears to have occurred as a drape over hilly paleotopography. The

most visible paleotopography is marked by the SR2 (MIS 5) paleosols. Due to the active seismicity of the region, we cannot exclude abrupt variations related to changes in paleotopography or postgenetic offsets of stratigraphic markers outside the investigated sections.

Our paleopedological data, together with the palynological record, allow the first robust interpretations to be made for MIS 5 paleoenvironments at Remizovka. The Bw horizon in SR2S2 (MIS 5e) resembles the lower part of interglacial pedocomplexes found in the Danube loess east of the Bohemian Massif, for example the Stillfried A pedocomplex near Vienna; there, the loamy brown horizon without signs of clay illuviation is interpreted as representing a soil formed under a temperate to Mediterranean climate (Fink, 1956, 1962). At Remizovka, the Bw horizon is less intensively developed and appears as a decalcified subsoil horizon of a degraded fossil Chernozem. Dark humic soils with numerous krotovina are typical in steppe ecosystems (Bronger, 1976). Indications of steppe conditions are consistent with the palynological data from Nigmatova (2009). Nevertheless, the paleoecological conditions for the genesis of the well-structured B_{ck} horizons remain to be established. From the present study, we exclude the formation of B_t horizons at Remizovka, which would have indicated strongly weathered forest soils, although such soils do occur in the LPS of Tadjikistan (Bronger et al., 1998a) and northern Iran (Vlaminck et al., 2016).

The luminescence ages from this study and those of Fitzsimmons et al. (in press) indicate high dust accumulation rates during MIS 4 and 3, although the precise timing of the peak phases remains to be established. The granulometric data of Machalett et al. (2008) indicate undisturbed, semi-continuous aeolian dust sedimentation after MIS 5. It is unclear to what extent the slope and paleotopography changed across the hill after MIS 5 and during the high loess flux phase of MIS 4, and to what degree this changed during MIS 3 and MIS 2. No visible stratigraphic markers can be traced in the LPS above this complex but, based on increased loess accumulation rates relative to the limited lateral space between the different profiles, we infer the formation of a positive loess landform comparable with “gredas” such as those visible at LPS Nusloch in Germany (Antoine et al., 2001).

Loess deposition may have experienced a similar peak in the region during MIS 2, accumulating elsewhere along the piedmont and simply not at Remizovka. Such a complex pattern of spatiotemporal variation in loess distribution is also reported from the lower Danube basin of Romania (Fitzsimmons, 2017). Studies from the Chinese part of the Ili basin indicate that loess accumulation peaks are not coeval between sites (Li et al., 2016a). Localized paleoclimatic and geomorphological influences must be invoked to explain these discrepancies.

Regional implications of this study

Thick loess deposits occur in various geomorphic contexts along the Zailisky Alatau piedmont. They often appear to drape pre-existing topography rather than occurring as a loess plateau. Previous estimations of thicknesses exceeding 100 m

need to be ground-truthed by boreholes and geophysical prospecting. From the one LPS studied in detail, Remizovka, we cannot determine mass accumulation rates for the entire Tian Shan piedmont with any accuracy. The timing of peaks in dust accumulation rates from the Ili basin loess clearly varies from site to site (Li et al., 2015, 2016a, 2016b; Song et al., 2015). This variability may be related to both differences in local geomorphic setting and (paleo)topographic variations. Regional mass accumulation rates must be interpreted carefully and require detailed surveys and high resolution geochronological data (Li et al., 2016a).

Deposits of thick loess in the Central Asian high mountain piedmont appear to be related to specific topographic positions. Although little data are available, the thickest loess in Central Asia appears to occur in the Vakhsh valley of the southern Tajik depression, where it appears to form a plateau-loess-like deposit (Dodonov, 1991; Bronger et al., 1998a, 1998b; Ding et al., 2002b). Substantial accumulation in this region may be related to its sheltered position, creating a dead-end for dust-bearing westerly winds (Vandenberghe et al., 2006). By comparison, the Ili basin of southeast Kazakhstan and far western China is relatively enclosed. Other than two localities of high loess accumulation in the northern (up to 200 m) and eastern (up to 100 m) Ili Basin (Fig. 1B; Song et al., 2014), there is as yet little evidence for the occurrence of plateau-like deposition in this area (Li et al., 2015).

However, even in the case of loess plateaus, paleotopography is likely to have been an influence and needs to be considered more carefully (Stevens et al., 2007; Fitzsimmons et al., 2013; Vandenberghe et al., 2014; Fitzsimmons, 2017). Loess plateaus experiencing high accumulation rates, such as in China (Liu, 1988; An et al., 1990; Ding et al., 2002a; Porter, 2013) or the Middle and Lower Danube Basin (Marković et al., 2011; Fitzsimmons et al., 2012; Buggle et al., 2014; Marković et al., 2015), are the exception to the rule. There are several loess regions worldwide, such as the Great Plains of the USA (Ruhe et al., 1967; Mason et al., 2007) or the Russian Plain (Velichko, 1990; Makeev, 2009), where horizontal drapes intersect with areas experiencing greater influence of (paleo)topography.

Landscapes with discontinuous loess cover of varying thickness due to variable topography are widespread in the temperate zone, such as in the patchy loess belt of Central Europe (Bertran et al., 2016), close to last glacial inland ice margins (Schaeztl et al., in press) or in parts of the Central Asian piedmont, e.g., the Ili Basin. Polygenetic loess profiles influenced by slope processes are abundant records of the complex landscape response to climatic changes (Sprafke, 2016). Consideration of paleotopography in loess research is not new (Ruhe et al., 1967), but has become somewhat overlooked in the search for thick, presumed complete, or representative sections.

Nevertheless, the LPS Remizovka appears to be exceptional, at least for the Kazakh part of the Ili Basin. This exposure, one of the northern Tian Shan's thickest loess deposits, provides a unique opportunity to investigate loess systems over three dimensions in time, combining the

potential of vertical drilling with detailed field descriptions of paleotopography in exposure.

In general, proper usage of terrestrial archives requires adequate documentation of the field context of the studied profile and a justification as to why the location was chosen. Complex terrestrial archives like LPS are not simply sampling sites for potential proxy data, but provide important field evidence by themselves. Pedology, sedimentology, geomorphology, and paleotopography all need to be considered as fundamental bases of understanding the loess archive before sampling for proxies of past climate reconstruction can begin (cf. Sprafke, 2016). Crucial elements of field documentation include precise coordinates and consistent stratigraphic description using standardized codes, all of which need to be unified and further developed within the loess community. Based on the fundamental paleopedological work of Bronger (1976, 2003; Bronger et al., 1998a), Sprafke (2016) applied a refined classification scheme based on color measurements and pedological designations of all units within a LPS, which has already been applied at Remizovka (Fitzsimmons et al., in press). Next to detailed descriptions, photos need to include various spatial scales from the landscape, to the outcrop, profile, feature, and its detail. Such information, together with laboratory data, must be made available in online supplements of the publication or in independent databases.

CONCLUSIONS

Current urban development at the LPS Remizovka highlights the importance of documenting this key regional archive of Pleistocene paleoclimatic evolution. This involves the review of previous work undertaken at outcrops that were destroyed during construction of the racing track. Despite limited documentation, we can rely on the few archival photos available, as well as Google Earth and Corona satellite imagery, to reconstruct the location of previously studied loess profiles. Using the published data and our own investigations on the MIS 5 pedocomplex, we were able to correlate these previously studied profiles, thereby resolving previous complications and furthering our understanding of the local and regional (paleo)topographic context.

Preliminary paleoenvironmental reconstructions point to hilly topography and a steppe ecosystem during MIS 5, interrupted by a phase of increased loess deposition. Future studies must address the paleopedological record of the LPS Remizovka, especially the paleoenvironmental significance of the well-structured BCK horizons in the lower part of the two pedocomplexes. From the chronological data in this study, we infer that sedimentation and pedogenesis may be not have been in phase with even and odd marine isotope stages, respectively, as is the case for loess records in Europe and China. High dust accumulation rates are evident during MIS 4 and 3, and may have led to landform growth. Future studies should address this unique paleoclimatic archive with a focused approach to reconstruct its formation and provide a consistent chronological framework. Drilling in front of the

main profile can complement the exposed outcrop. In sum, our study stresses the general need to adequately consider (paleo)topography in the interpretations of LPS, and to provide comprehensive documentation and datasets.

ACKNOWLEDGMENTS

We thank Robert Peticzka (University of Vienna) for providing the spectrophotometer and Leonor Rodrigues (University of Bern, CNRS Montpellier) for the grain size measurements. Radu Iovita (New York University) is thanked for providing photos from 2013. Corona and SRTM data are distributed by the Land Processes Distributed Active Archive Center (LP DAAC), located at USGS/EROS, Sioux Falls, SD <http://lpdaac.usgs.gov>. Pléiades stereo imagery was acquired with a grant from the NERC/ESRC Earthquake without Frontiers Project (EwF; grant code: EwF_NE/J02001X/1_1). We gratefully acknowledge the thoughtful review comments of an anonymous reviewer and Joe Mason. Thanks also to guest editor Randy Schaetzl and Nicholas Lancaster for providing valuable suggestions that improved the final version of this manuscript.

SUPPLEMENTARY MATERIALS

To view supplementary material for this article, please visit <https://doi.org/10.1017/qua.2017.103>

REFERENCES

- Abdrakhmatov, K.E., Walker, R.T., Campbell, G.E., Carr, A.S., Elliott, A., Hillemann, C., Hollingsworth, J., et al., 2016. Multisegment rupture in the 11 July 1889 Chilik earthquake (M-w 8.0-8.3), Kazakh Tien Shan, interpreted from remote sensing, field survey, and paleoseismic trenching. *Journal of Geophysical Research-Solid Earth* 121, 4615–4640.
- Adamiec, G., Aitken, M., 1998. Dose-rate conversion factors: update. *Ancient TL* 16, 37–50.
- An, Z.S., Liu, T.S., Porter, S.C., Kukla, G.J., Wu, X.H., Hua, Y.M., 1990. The long-term paleomonsoon variation record by the loess-paleosol sequence in central China. *Quaternary International* 7/8, 91–95.
- Ankjærgaard, C., Guralnik, B., Buylaert, J.P., Reimann, T., Yi, S.W., Wallinga, J., 2016. Violet stimulated luminescence dating of quartz from Luochuan (Chinese loess plateau): agreement with independent chronology up to ~600 ka. *Quaternary Geochronology* 34, 33–46.
- Antoine, P., Rousseau, D.D., Moine, O., Kunesch, S., Hatté, C., Lang, A., Tissoux, H., Zöller, L., 2009. Rapid and cyclic aeolian deposition during the Last Glacial in European loess: a high-resolution record from Nussloch, Germany. *Quaternary Science Reviews* 28, 2955–2973.
- Antoine, P., Rousseau, D.D., Zöller, L., Lang, A., Munaut, A.V., Hatté, C., Fontugne, M., 2001. High-resolution record of the last Interglacial-glacial cycle in the Nussloch loess-paleosol sequences, Upper Rhine Area, Germany. *Quaternary International* 76–7, 211–229.
- Atrushkevitch, P.A., Kalabaev, N.B., Kartashov, A.P., Lototsky, V. D., Ostropico, P.A., 1988. Research on crustal movements on the Alma-Ata polygon, Northern Tien Shan. *Journal of Geodynamics* 9, 279–292.

- Auclair, M., Lamothe, M., Huot, S., 2003. Measurement of anomalous fading for feldspar IRSL using SAR. *Radiation Measurements* 37, 487–492.
- Bertran, P., Liard, M., Sitzia, L., Tissoux, H., 2016. A map of Pleistocene aeolian deposits in Western Europe, with special emphasis on France. *Journal of Quaternary Science* 31, 844–856.
- Bronger, A., 1976. *Zur quartären Klima- und Landschaftsentwicklung des Karpatenbeckens auf (paläo-)pedologischer und bodengeographischer Grundlage*. Geographisches Institut, Universität Kiel, Kiel.
- Bronger, A., 2003. Correlation of loess-paleosol sequences in East and Central Asia with SE Central Europe: towards a continental Quaternary pedostratigraphy and paleoclimatic history. *Quaternary International* 106, 11–31.
- Bronger, A., Winter, R., Heinkele, T., 1998a. Pleistocene climatic history of East and Central Asia based on paleopedological indicators in loess-paleosol sequences. *Catena* 34, 1–17.
- Bronger, A., Winter, R., Sedov, S., 1998b. Weathering and clay mineral formation in two Holocene soils and in buried paleosols in Tadjikistan: towards a Quaternary paleoclimatic record in Central Asia. *Catena* 34, 19–34.
- Buggle, B., Hambach, U., Kehl, M., Marković, S.B., Zöller, L., Glaser, B., 2013. The progressive evolution of a continental climate in southeast-central European lowlands during the middle Pleistocene recorded in loess paleosol sequences. *Geology* 41, 771–774.
- Buggle, B., Hambach, U., Müller, K., Zöller, L., Marković, S.B., Glaser, B., 2014. Iron mineralogical proxies and Quaternary climate change in SE-European loess-paleosol sequences. *Catena* 117, 4–22.
- Buylaert, J.-P., Jain, M., Murray, A.S., Thomsen, K.J., Thiel, C., Sohbati, R., 2012a. A robust feldspar luminescence dating method for Middle and Late Pleistocene sediments. *Boreas* 41, 435–451.
- Buylaert, J.P., Jain, M., Murray, A.S., Thomsen, K.J., Thiel, C., Sohbati, R., 2012b. A robust feldspar luminescence dating method for Middle and Late Pleistocene sediments. *Boreas* 41, 435–451.
- Chen, Q., Liu, X.M., Heller, F., Hirt, A.M., Lu, B., Guo, X.L., Mao, X.G., et al., 2012. Susceptibility variations of multiple origins of loess from the Ily Basin (NW China). *Chinese Science Bulletin* 57, 1844–1855.
- de Lussy, F., Kubik, P., Greslou, D., Pascal, V., Gigord, P., Cantou, J.P., 2005. PLEIADES-HR image system products and quality-PLEIADES-HR image system products and geometric accuracy. Proceedings of the International Society for Photogrammetry and Remote Sensing Workshop, Hannover, Germany, 17–20 May.
- Delvaux, D., Abdrakhmatov, K.E., Lemzin, I.N., Strom, A.L., 2001. Landslide and surface breaks of the 1911 M 8.2 Kemin Earthquake. *Landslides* 42, 1583–1592.
- Ding, Z.L., Derbyshire, E., Yang, S.L., Yu, Z.W., Xiong, S.F., Liu, T.S., 2002a. Stacked 2.6-Ma grain size record from the Chinese loess based on five sections and correlation with the deep-sea $\delta^{18}\text{O}$ record. *Paleoceanography* 17, 5–1–5–21.
- Ding, Z.L., Ranov, V., Yang, S.L., Finaev, A., Han, J.M., Wang, G.A., 2002b. The loess record in southern Tajikistan and correlation with Chinese loess. *Earth and Planetary Science Letters* 200, 387–400.
- Dodonov, A., 1991. Loess of Central Asia. *GeoJournal* 24, 185–194.
- Dodonov, A.E., Baiguzina, L.L., 1995. Loess stratigraphy of Central Asia: palaeoclimatic and palaeoenvironmental aspects. *Quaternary Science Reviews* 14, 707–720.
- Dodonov, A.E., Sadchikova, T.A., Sedov, S.N., Simakova, A.N., Zhou, L.P., 2006. Multidisciplinary approach for paleoenvironmental reconstruction in loess-paleosol studies of the Darai Kalon section, Southern Tajikistan. *Quaternary International* 152, 48–58.
- E, C.Y., Lai, Z.P., Sun, Y.J., Hou, S.S., Yu, L.P., Wu, C.Y., 2012. A luminescence dating study of loess deposits from the Yili River basin in western China. *Quaternary Geochronology* 10, 50–55.
- Feng, Z.D., Ran, M., Yang, Q.L., Zhai, X.W., Wang, W., Zhang, X.S., Huang, C.Q., 2011. Stratigraphies and chronologies of late Quaternary loess-paleosol sequences in the core area of the central Asian arid zone. *Quaternary International* 240, 156–166.
- Fink, J., 1956. Zur Korrelation der Terrassen und Lössen in Österreich. *Eiszeitalter und Gegenwart* 7, 49–77.
- Fink, J., 1962. Studien zur absoluten und relativen Chronologie der fossilen Böden in Österreich. II. Wetzleinsdorf und Stillfried. *Archaeologia Austriaca* 31, 1–18.
- Fink, J., 1976. *Exkursion durch den österreichischen Teil des nördlichen Alpenvorlandes und den Donauraum zwischen Krems und der Wiener Pforte*. ÖAW, Wien.
- Fitzsimmons, K.E., 2017. Reconstructing palaeoenvironments on desert margins: new perspectives from Eurasian loess and Australian dry lake shorelines. *Quaternary Science Reviews* 171, 1–19.
- Fitzsimmons, K.E., Hambach, U., Veres, D., Iovita, R., 2013. The Campanian Ignimbrite eruption: new data on volcanic ash dispersal and its potential impact on human evolution. *PLoS ONE* 8, e65839. <http://dx.doi.org/10.1371/journal.pone.0065839>.
- Fitzsimmons, K.E., Marković, S.B., Hambach, U., 2012. Pleistocene environmental dynamics recorded in the loess of the middle and lower Danube basin. *Quaternary Science Reviews* 41, 104–118.
- Fitzsimmons, K.E., Sprafke, T., Zielhofer, C., Günter, C., Deom, J.-M., Sala, R., Iovita, R., in press. Loess accumulation in the Tian Shan piedmont: implications for palaeoenvironmental change in arid Central Asia. *Quaternary International* (in press).
- Food and Agriculture Organization of the United Nations (FAO), 2006. *Guidelines for Soil Description*. 4th ed. Food and Agriculture Organization of the United Nations, Rome.
- Frechen, M., Schweitzer, U., Zander, A., 1996. Improvements in sample preparation for the fine grain technique. *Ancient TL* 14, 15–17.
- Galbraith, R.F., Roberts, R.G., Laslett, G.M., Yoshida, H., Olley, J.M., 1999. Optical dating of single and multiple grains of quartz from Jinnium rock shelter, northern Australia. Part 1, Experimental design and statistical models. *Archaeometry* 41, 339–364.
- Jain, M., Buylaert, J.P., Thomsen, K.J., Murray, A.S., 2015. Further investigations on ‘non-fading’ in K-Feldspar. *Quaternary International* 362, 3–7.
- Kang, S.G., Wang, X.L., Lu, Y.C., Liu, W.G., Song, Y.G., Wang, N., 2015. A high-resolution quartz OSL chronology of the Taled loess over the past similar to 30 ka and its implications for dust accumulation in the Ili Basin, Central Asia. *Quaternary Geochronology* 30, 181–187.
- Konert, M., Vandenberghe, J.E.F., 1997. Comparison of laser grain size analysis with pipette and sieve analysis: a solution for the underestimation of the clay fraction. *Sedimentology* 44, 523–535.
- Koppes, M., Gillespie, A.R., Burke, R.M., Thompson, S.C., Stone, J., 2008. Late Quaternary glaciation in the Kyrgyz Tien Shan. *Quaternary Science Reviews* 27, 846–866.

- Kukla, G.J., 1987. Loess Stratigraphy in Central China. *Quaternary Science Reviews* 6, 191–219.
- Kukla, G.J., An, Z.S., Melice, J.L., Gavin, J., Xiao, J.L., 1990. Magnetic-Susceptibility Record of Chinese Loess. *Transactions of the Royal Society of Edinburgh-Earth Sciences* 81, 263–288.
- Landgraf, A., Dzhumabaeva, A., Abdrakhmatov, K.E., Strecker, M.R., Macaulay, E.A., Arrowsmith, J.R., Sudhaus, H., Preusser, F., Rugel, G., Merchel, S., 2016. Repeated large-magnitude earthquakes in a tectonically active, low-strain continental interior: the northern Tien Shan, Kyrgyzstan. *Journal of Geophysical Research-Solid Earth* 121, 3888–3910.
- Lauer, T., Vlaminc, S., Frechen, M., Rolf, C., Kehl, M., Sharifi, J., Lehdorff, E., Khormali, F., 2017. The Agh Band loess-palaeosol sequence – a terrestrial archive for climatic shifts during the last and penultimate glacial–interglacial cycles in a semiarid region in northern Iran. *Quaternary International* 429, 13–30.
- Lehmkuhl, F., Zens, J., Krauss, L., Schulte, P., Kels, H., 2016. Loess-paleosol sequences at the northern European loess belt in Germany: distribution, geomorphology and stratigraphy. *Quaternary Science Reviews* 153, 11–30.
- Li, G.Q., Rao, Z.G., Duan, Y.W., Xia, D.S., Wang, L.B., Madsen, D.B., Jia, J., et al., 2016a. Paleoenvironmental changes recorded in a luminescence dated loess/paleosol sequence from the Tianshan Mountains, arid central Asia, since the Penultimate Glaciation. *Earth and Planetary Science Letters* 448, 1–12.
- Li, Y., Song, Y.G., Lai, Z.P., Han, L., An, Z.S., 2016b. Rapid and cyclic dust accumulation during MIS 2 in Central Asia inferred from loess OSL dating and grain-size analysis. *Scientific Reports* 6, 32365. <http://dx.doi.org/10.1038/srep32365>.
- Li, Y., Song, Y.G., Yan, L.B., Chen, T., An, Z.S., 2015. Timing and Spatial Distribution of Loess in Xinjiang, NW China. *PLoS ONE*, 10. <http://dx.doi.org/10.1371/journal.pone.0125492>.
- Liu, T.S., 1988. *Loess in China*. 2nd ed. Springer-Verlag, Berlin.
- Machalett, B., Frechen, M., Hambach, U., Oches, E.A., Zöller, L., Marković, S.B., 2006. The loess sequence from Remisowka (northern boundary of the Tien Shan Mountains, Kazakhstan) - Part I: Luminescence dating. *Quaternary International* 152–153, 192–201.
- Machalett, B., Oches, E.A., Frechen, M., Zöller, L., Hambach, U., Mavlyanova, N.G., Marković, S.B., Endlicher, W., 2008. Aeolian dust dynamics in central Asia during the Pleistocene: driven by the long-term migration, seasonality, and permanency of the Asiatic polar front. *Geochemistry Geophysics Geosystems* 9, 1–22.
- Makeev, A.O., 2009. Pedogenic alteration of aeolian sediments in the upper loess mantles of the Russian Plain. *Quaternary International* 209, 79–94.
- Marković, S.B., Fitzsimmons, K.E., Sprafke, T., Gavrilovic, D., Smalley, I.J., Jovic, V., Svircev, Z., Gavrilov, M.B., Beslin, M., 2016. The history of Danube loess research. *Quaternary International* 399, 86–99.
- Marković, S.B., Hambach, U., Stevens, T., Kukla, G.J., Heller, F., McCoy, W.D., Oches, E.A., Buggle, B., Zöller, L., 2011. The last million years recorded at the Stari Slankamen (Northern Serbia) loess-palaeosol sequence: revised chronostratigraphy and long-term environmental trends. *Quaternary Science Reviews* 30, 1142–1154.
- Marković, S.B., Stevens, T., Kukla, G.J., Hambach, U., Fitzsimmons, K.E., Gibbard, P.L., Buggle, B., et al., 2015. Danube loess stratigraphy — towards a pan-European loess stratigraphic model. *Earth-Science Reviews* 148, 228–258.
- Mason, J.A., Joeckel, R.M., Bettis, E.A. III, 2007. Middle to Late Pleistocene loess record in eastern Nebraska, USA, and implications for the unique nature of Oxygen Isotope Stage 2. *Quaternary Science Reviews* 26, 773–792.
- Narama, C., Kaab, A., Duishonakunov, M., Abdrakhmatov, K., 2010. Spatial variability of recent glacier area changes in the Tien Shan Mountains, Central Asia, using Corona (similar to 1970), Landsat (similar to 2000), and ALOS (similar to 2007) satellite data. *Global and Planetary Change* 71, 42–54.
- Nigmatova, S., 2009. First results of palynological researches of Late Pleistocene and Holocene Loess Kazakhstan (North Tian-Shan). NSF Collaborative research: bioclimatic reconstruction of the past 50,000 years from eolian sequences in westerlies-dominated Central Asia, 2006–2008. Unpublished project report, Louisiana State University.
- Owen, L.A., Dortch, J.M., 2014. Nature and timing of Quaternary glaciation in the Himalayan-Tibetan orogen. *Quaternary Science Reviews* 88, 14–54.
- Porter, S.C., 2013. Loess Records - China. In Elias, S.A., Mock, C.J. (Eds.), *Encyclopedia of Quaternary Science*. 2nd ed. Elsevier, Amsterdam, pp. 595–605.
- Prescott, J.R., Hutton, J.T., 1994. Cosmic ray contributions to dose rates for luminescence and ESR dating: large depths and long term variations. *Radiation Measurements* 23, 497–500.
- Ran, M., Feng, Z.D., 2014. Variation in carbon isotopic composition over the past ca. 46,000 yr in the loess–paleosol sequence in central Kazakhstan and paleoclimatic significance. *Organic Geochemistry* 73, 47–55.
- Rees-Jones, J., Tite, M.S., 1997. Optical dating results for British archaeological sediments. *Archaeometry* 36, 177–187.
- Roberts, H.M., 2008. The development and application of luminescence dating to loess deposits: a perspective on the past, present and future. *Boreas* 37, 483–507.
- Rousseau, D.D., Antoine, P., Kunesch, S., Hatté, C., Rossignol, J., Packman, S., Lang, A., Gauthier, C., 2007. Evidence of cyclic dust deposition in the US Great plains during the last deglaciation from the high-resolution analysis of the Peoria Loess in the Eustis sequence (Nebraska, USA). *Earth and Planetary Science Letters* 262, 159–174.
- Ruhe, R.V., Daniels, R.B., Cady, J.G., 1967. *Landscape Evolution and Soil Formation in Southwestern Iowa*. U.S. Department of Agriculture, Washington, DC.
- Schaetzl, R.J., Larson, P.H., Faulkner, D.J., Running, G.L., Jol, H.M., Rittenour, T.M., in press. Eolian Sand and Loess Deposits Indicate West-Northwest Paleowinds During the Late Pleistocene in Western Wisconsin, USA. *Quaternary Research* (In Press).
- Schirmer, W., 2012. Rhine loess at Schwalbenberg II - MIS 4 and 3. *E & G Quaternary Science Journal* 61, 32–47.
- Schulte, P., Sprafke, T., Rodrigues, L., Fitzsimmons, K.E., in press. Are fixed grain size ratios useful proxies for loess sedimentation dynamics? Experiences from Remizovka, Kazakhstan. *Aeolian Research* (In Press).
- Sedov, S., Sycheva, S., Pi, T., Díaz, J., 2013. Last Interglacial paleosols with Argic horizons in Upper Austria and Central Russia: pedogenetic and paleoenvironmental inferences from comparison with the Holocene analogues. *E&G Quaternary Science Journal* 62, 44–58.
- Selander, J., Oskin, M., Ormukov, C., Abdrakhmatov, K., 2012. Inherited strike-slip faults as an origin for basement-cored uplifts: example of the Kungey and Zailikey ranges, northern Tian Shan. *Tectonics*, 31. <http://dx.doi.org/10.1029/2011TC003002>.

- Smalley, I.J., Krinsley, D.H., 1978. Loess deposits associated with deserts. *Catena* 5, 53–66.
- Smalley, I.J., Mavlyanova, N.G., Rakhmatullaev, K.L., Shermatov, M.S., Machalet, B., Dhand, K.O., Jefferson, I.F., 2006. The formation of loess deposits in the Tashkent region and parts of Central Asia; and problems with irrigation, hydrocollapse and soil erosion. *Quaternary International* 152, 59–69.
- Song, Y.G., Chen, X.L., Qian, L.B., Li, C.X., Li, Y., Li, X.X., Chang, H., An, Z.S., 2014. Distribution and composition of loess sediments in the Ili Basin, Central Asia. *Quaternary International* 334, 61–73.
- Song, Y.G., Lai, Z.P., Li, Y., Chen, T., Wang, Y.X., 2015. Comparison between luminescence and radiocarbon dating of late Quaternary loess from the Ili Basin in Central Asia. *Quaternary Geochronology* 30, 405–410.
- Song, Y.G., Li, C.X., Zhao, J.D., Cheng, P., Zeng, M.X., 2012. A combined luminescence and radiocarbon dating study of the Ili loess, Central Asia. *Quaternary Geochronology* 10, 2–7.
- Sprafke, T., 2016. *Löss in Niederösterreich - Archiv quartärer Klima- und Landschaftsveränderungen*. Würzburg University Press, Würzburg.
- Sprafke, T., Obrecht, I., 2016. Loess: rock, sediment or soil - what is missing for its definition? *Quaternary International* 399: 198–207.
- Sprafke, T., Thiel, C., Terhorst, B., 2014. From micromorphology to palaeoenvironment: the MIS 10 to MIS 5 record in Paudorf (Lower Austria). *Catena* 117, 60–72.
- Stevens, T., Thomas, D.S.G., Armitage, S.J., Lunn, H.R., Lu, H.Y., 2007. Reinterpreting climate proxy records from late Quaternary Chinese loess: a detailed OSL investigation. *Earth-Science Reviews* 80, 111–136.
- Sun, Y.B., An, Z.S., Clemens, S.C., Bloemendal, J., Vandenberghe, J., 2010. Seven million years of wind and precipitation variability on the Chinese Loess Plateau. *Earth and Planetary Science Letters* 297, 525–535.
- Tatevossian, R.E., 2007. The Verny, 1887, earthquake in Central Asia: application of the INQUA scale, based on coseismic environmental effects. *Quaternary International* 173–174: 23–29.
- Thiel, C., Buylaert, J.P., Murray, A.S., Terhorst, B., Hofer, I., Tsukamoto, S., Frechen, M., 2011. Luminescence dating of the Stratzing loess profile (Austria) - testing the potential of an elevated temperature post-IR IRSL protocol. *Quaternary International* 234, 23–31.
- Thiel, C., Horváth, E., Frechen, M., 2014. Revisiting the loess/palaeosol sequence in Paks, Hungary: a post-IR IRSL based chronology for the ‘Young Loess Series’. *Quaternary International* 319, 88–98.
- Vandenberghe, J., Marković, S.B., Jovanović, M., Hambach, U., 2014. Site-specific variability of loess and palaeosols (Ruma, Vojvodina, northern Serbia). *Quaternary International* 334–335, 86–93.
- Vandenberghe, J., Renssen, H., van Huissteden, K., Nugteren, G., Konert, M., Lu, H.Y., Dodonov, A., Buylaert, J.-P., 2006. Penetration of Atlantic westerly winds into Central and East Asia. *Quaternary Science Reviews* 25, 2380–2389.
- Vasiljević, D.A., Marković, S.B., Hose, T.A., Ding, Z.L., Guo, Z.T., Liu, X.M., Smalley, I.J., Lukić, T., Vujičić, M.D., 2014. Loess-palaeosol sequences in China and Europe: common values and geoconservation issues. *Catena* 117, 108–118.
- Velichko, A.A., 1990. Loess-paleosol formation on the Russian Plain. *Quaternary International* 7–8, 103–114.
- Vlaminck, S., Kehl, M., Lauer, T., Shahriari, A., Sharifi, J., Eckmeier, E., Lehndorff, E., Khormali, F., Frechen, M., 2016. Loess-soil sequence at Toshan (Northern Iran): insights into late Pleistocene climate change. *Quaternary International* 399, 122–135.
- Vogel, J.C., Zagwijn, W.H., 1967. Groningen radiocarbon dates VI. *Radiocarbon* 9, 63–106.
- Weather and Climate. 2017. Climate Almaty (accessed April 07 2017). [In Russian]. <http://www.pogodaiklimat.ru/climate/36870.htm>.
- Youn, J.H., Seong, Y.B., Choi, J.H., Abdrakhmatov, K., Ormukov, C., 2014. Loess deposits in the northern Kyrgyz Tien Shan: implications for the paleoclimate reconstruction during the Late Quaternary. *Catena* 117, 81–93.
- Zech, R., Zech, M., Marković, S., Hambach, U., Huang, Y.S., 2013. Humid glacials, arid interglacials? Critical thoughts on pedogenesis and paleoclimate based on multi-proxy analyses of the loess-palaeosol sequence Crvenka, Northern Serbia. *Palaeogeography, Palaeoclimatology, Palaeoecology* 387, 165–175.